



Effect of Variation in Mass Composition of TiO₂/Activated Carbon Cassava Peel Effect on Crystal Size and Structure

Faadhilah Fauziyah¹, Yenni Darvina^{1*}, Ratnawulan¹, Gusnedi¹

¹ Department of Physics, Universitas Negeri Padang, Padang 25131, Indonesia

Article History

Received : February, 10th 2024

Revised : February, 25th 2024

Accepted : March 31st, 2024

Published : March 31st, 2024

DOI:

<https://doi.org/10.24036/jeap.v2i1.45>

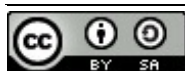
Corresponding Author

*Author Name: Yenni Darvina

Email: ydarvina@fmipa.unp.ac.id

Abstract: Battery is a device that can convert the chemical energy into electrical energy which can be used by an electronic device. Almost all portable electronic devices such as cellphones, laptops, flashlights, and remote controls use batteries as their power source. The working indicator of a battery is its capacity, its electrochemical cycling ability depends on the anode material. In general, battery anodes are made using graphite. However, graphite has limitations, namely the ease of short-circuiting. Because graphite has limitations, a graphite substitute will be made from a TiO₂ nanocomposite with activated carbon. Nanocomposites are new materials that are formed through the combination of two or more compounds so as to produce a new property and have a nano size. TiO₂ is used because it can reduce short cycles, good stability, high current density and can increase battery performance capacity. Activated carbon is used in order to expand the surface of the material to get a large capacitance. The activated carbon used in this article is cassava peel from waste that has not been utilized in order to reduce environmental pollution and can add economic value to the waste. The purpose of this research is to produce TiO₂/Active carbon nanocomposites to be tested for structure and crystal size using XRD. TiO₂/Active carbon nanocomposites were obtained using the sol-gel method. Variations in the mass composition of TiO₂/Activated carbon used are 40%:60%, 50%:50%, and 60%:40%. Based on the tests that have been carried out, the smallest crystal size obtained in the 40%: 60% variation is 58.4 nm with a Tetragonal structure for TiO₂ while Cubic and Rhombohedral for carbon.

Keywords: Activated Carbon, Crystal Size, Crystal Structure, Nanocomposite, TiO₂.



Journal of Experimental and Applied Physics is an open access article licensed under a Creative Commons Attribution ShareAlike 4.0 International License which permits unrestricted use, distribution, and reproduction in any medium, provided the original work is properly cited. ©2024 by author.

1. Introduction

Nowadays, almost all electronic items use batteries, because batteries are a reliable source of electricity for electronic goods that are portable and can be carried anywhere [1]. Because of the

How to cite:

F. Fauziyah, Y. Darvina, Ratnawulan, and Gusnedi, 2024, Mass Composition of TiO₂/Activated Carbon Cassava Peel Effect on Crystal Size and Structur, *Journal of Experimental and Applied Physics*, Vol.2, No.1, page 35-47.

large demand for batteries, of course we want a battery that is in good condition, such as one that doesn't heat up quickly and doesn't have the potential for short circuits. A battery is a tool used to store electrical energy to obtain an electric current so that it can be used to power remotes, cellphones, laptops, cameras and other electronic items [2][3][4]. The working indicator of a battery is capacity, its electrochemical cycling capability depends on the anode material [5]. In general, battery anodes are made using graphite. However, graphite has limitations, namely that it can easily cause short circuits [6]. Because graphite has limitations, a replacement for graphite from TiO₂ nanocomposites with activated carbon will be made.

In recent times, the development of nanoparticles has led to the development of nanocomposites. Nanocomposites are new materials that are formed by combining two or more compounds to produce new properties and have a nano size with the aim of having better properties. [7][8][9][10]. Nanocomposites can be considered as solid structures with nanometer-scale dimensions that repeat at different distances between the constituent shapes of the structure [11]. A nanometer is one thousandth of a micrometer, or one millionth of a millimeter, or one billionth of a meter [12]. Materials of this type consist of inorganic solids composed of organic components. Apart from that, nanocomposite materials can also consist of two or more inorganic/organic molecules in several forms of combination with a barrier between them of at least one molecule or have nano-sized characteristics. The bonds between particles that occur in nanocomposite materials play an important role in enhancing and limiting material properties. These nano-sized particles have a high interaction surface area. The more particles that interact, the stronger the material [13]. This is what makes the bonds between particles stronger so that the mechanical properties of the material increase.

One example of a nanocomposite that can be taken is the TiO₂/Cassava peel activated carbon nanocomposite. Nanocomposites are receiving serious attention from researchers to produce new products and innovations that have high usability so that product modifications continue to emerge. This is caused by composite materials which are needed in all fields, one example is in the electronics field. This article will examine the manufacture of TiO₂/Cassava peel activated carbon nanocomposites to determine the structure and crystal size. Titanium dioxide (TiO₂) is a photocatalyst material based on its semiconductor properties. TiO₂ is also non-toxic, has high thermal stability, and can be used repeatedly without losing its catalytic activity [14]. Titanium dioxide (TiO₂) is a white dioxide compound. TiO₂ is the most effective catalyst and is more often used than other types of catalysts [15]. TiO₂ is used because it can reduce short cycles, has good stability, high current density and can increase battery performance capacity [5]. The use of TiO₂ will be doped with activated carbon. Activated carbon is a porous material containing 85%-95% carbon with a large surface area [16][17]. Activated carbon is used to expand the surface of the material and to increase its absorption properties [5]. The adsorption/absorption capacity of activated carbon can be increased through the activation process so that the pores are open and the surface area is larger [18]. A large surface area will get a large capacitance value, and vice versa, a small surface area will also get a small capacitance value. [19]. The material used to make activated carbon is cassava peel. The percentage of cassava skin is approximately 20% of the tubers so that per kg of cassava tubers produces 0.2 kg of cassava skin [20]. Cassava peel contains quite high levels of carbon, cellulose, hemicellulose and lignin at 59.31%, 50%, 35% and 30% [21]. Cassava peel contains a carbon element of 59.31% so it can be used to make active carbon [22].

In research conducted by Zaldi & Ratnawulan (2021) entitled "The Effect of Composition Variations on Crystal Size of MnO-Fe₂O₃/PS Nanocomposite Layers as Self Cleaning", stated that variations in composition affect the structure and size of the crystals, where the crystal structure found was Cubic, Rhombohedral and Tetragonal, while the maximum crystal size obtained for MnO was 61.26 nm, Fe₂O was 50.45 nm, and MnO-Fe₂O was 53.08 nm [23]. In research conducted by Aflahannisa & Astuti (2016) entitled "Synthesis of Carbon-TiO₂ Nanocomposites as Lithium Battery Anodes", the results obtained were different crystal structures and sizes for each variation of Carbon-TiO₂ composition, namely variations of 5%:95% having a Rhombohedral structure for C and Tetragonal for TiO₂ with a crystal size of 66.89 nm, variations of 10%:90% have a Rhombohedral structure for C and Tetragonal for TiO₂ with a crystal size of 175.17 nm, variations of 15%:85% have a Hexagonal structure for C and Tetragonal for TiO₂ with a crystal size of 99.52 nm, and variations of 20%:80% has a Hexagonal structure for C and Tetragonal for TiO₂ with a crystal size of 44.76 nm [5]. In research conducted by Susana & Astuti (2016) entitled "The Effect of LiOH Concentration on the Electrical Properties of Candle Shell Activated Carbon-Based Lithium Battery Anodes", obtained the results of different crystal sizes for each variation of LiOH composition, namely a variation of 0.2 grams is 5,136,018,136 nm, 1 gram variation is 586,979,465 nm, and 1.5 gram variation is 5,870,281,736 nm [24].

Based on the background above, the problem formulation taken is how does cassava peel carbon, cassava peel activated carbon, TiO₂, and variations in the mass composition of the TiO₂/Cassava peel activated carbon nanocomposite affect the lattice constant, structure and crystal size?

2. Materials and Method

An experimental approach was used in making the TiO₂/Cassava peel activated carbon nanocomposite to determine how variations in the mass composition of the TiO₂/Cassava peel activated carbon nanocomposite affect the electrical properties. There are three variables that form this research, namely the independent variable, dependent variable, and control variable. Variations in the mass of the TiO₂/Activated Carbon cassava peel composite were the independent variables in this study. The structure and crystal size of TiO₂, carbon, activated carbon, and variations of TiO₂/Activated carbon cassava peel nanocomposites are the dependent variables. Then carbonization temperature, carbon activator, carbon activation time, carbon milling time, and nanocomposite synthesis process as control variables.

There are three stages in making activated carbon, the first is the dehydration stage, namely the sample is dried in an oven or under sunlight, the second is the carbonization stage, namely the dried sample is burned in a furnace at a predetermined temperature and time so that it becomes charcoal and then the charcoal crushed and sifted using a predetermined sieve size, and third is the activation stage, namely the sifted charcoal is soaked in the activator solution for a specified time [25]. In this research, the carbonization stage uses a temperature of 600⁰C for two hours, as in the research entitled "Utilization of Cassava Skin as Active Carbon Raw Material", in making active carbon from cassava skin with various carbonization temperatures from 300⁰C-600⁰C, producing active carbon which is carbonized at 600⁰C for two hours has the best absorption [26]. In this research, the activator used is NaCl, as in the research entitled "Characterization of Cassava Peel Activated Carbon (*Manihot utilisima*) with Varying Types of Activators", in making cassava peel

activated carbon with a variety of activators, the selected activator is used as an activator for quality characteristics. Cassava peel activated carbon is an activator of NaCl solution [16].

Nanocomposite materials will be made using the sol-gel method. The sol-gel method is a process for making inorganic materials through a chemical reaction in a solution at low temperatures. The sol-gel method is known as a fairly simple and easy nanoparticle synthesis method [27][28]. This method is a "wet method" because the process involves a solution as the medium. In the sol-gel method, as the name suggests, the solution undergoes a phase change to become a sol (a colloid that has solids suspended in the solution) and then becomes a gel (a colloid but has a larger solid fraction than the sol). In general, the sol-gel process involves the transition of the system from a liquid "sol" to a solid "gel".

The nanocomposite material that has been made will be tested for its crystal structure and size using XRD. X-ray Diffraction (XRD) is a tool used to analyze the phases of crystalline materials [29]. X-ray diffraction is an analytical method that utilizes the interaction between X-rays and atoms arranged in a crystal system [30]. The material to be analyzed can be in solid form, powder form or flour. By using XRD, we can find out the mineral content regarding the structure of the material or the value of the crystal angle. X-ray diffraction is an analytical method that utilizes the interaction between X-rays and atoms arranged in a crystal system [30].

The equipment used in this research was a furnace, mortar and pestle, high energy milling (HEM), pH paper, spatula, petri dish, digital balance, measuring cup, magnetic stirrer hot plate, porcelain cup, sample mold, and felt tool. The materials used in this research were cassava peel, 5% NaCl, distilled water, TiO₂, PEG 6000, ethanol, and PVC. The testing tool used in this research is X-ray Diffraction (XRD).

The process of making activated carbon begins by drying cassava skin under the heat of the sun and then carbonizing it in a furnace at a temperature of 600⁰C for 2 hours until it forms charcoal, the charcoal is crushed using a mortar and then 1 gram is set aside to be tested using XRD, after that the charcoal is soaked in a solution of NaCl 5 % for 24 hours then rinsed with distilled water until the pH is neutral, then the charcoal is dried in the oven at 120⁰ for 2 hours, the finished activated carbon is ground using HEM, and the activated carbon is then characterized using XRD [26].

The TiO₂/Activated Carbon nanocomposite synthesis stage was carried out using the sol-gel method by mixing TiO₂ with cassava peel activated carbon in successive ratios of 40%:60%, 50%:50%, and 60%:40% for a total of 3.2 grams. 45 grams of PEG 6000 is dissolved in 60 mL of 95% ethanol with a hot plate magnetic stirrer at a temperature of 50⁰C with a speed of 300 rpm until homogeneous then add TiO₂/Activated Carbon and add 4 molar citric acid until the pH is 4-5 then increase the temperature to 100⁰C at a speed of 1000 rpm for 1.5 hours to form a gel, the gel formed is calcined at 300⁰C until dry, the dry gel is smoothed using HEM, and the TiO₂/Activated Carbon nanocomposite has been formed and then prepared according to the required tests [31].

XRD testing can provide information about the structure and size of the crystal. The crystal size can be calculated using the Scherrer Equation (1) below [32].

$$D = \frac{k\lambda}{B \cos \theta} \quad (1)$$

where, D is the crystal size (nm), k is the material constant of 0.9, λ is the x-ray wavelength (nm), and B is the Bragg diffraction angle.

3. Results and Discussion

The results of characterization using XRD tools for the samples are described as follows. The following is TiO_2 characterization data using an XRD tool.

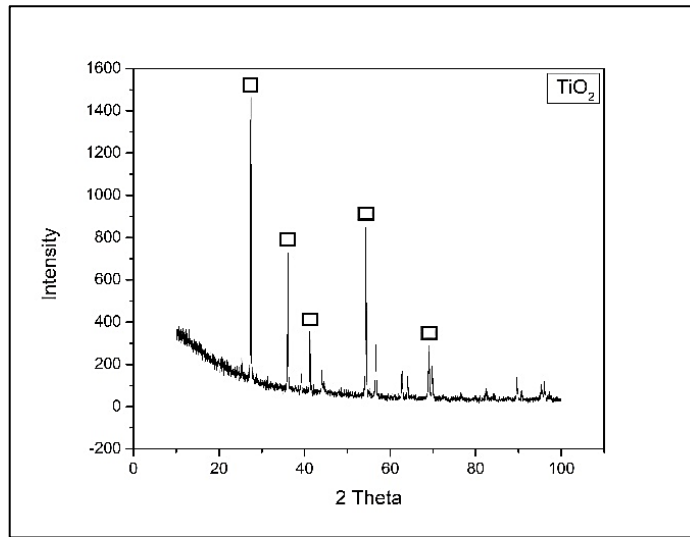


Figure 1. TiO_2 diffraction pattern

Figure 1 is a graph of the diffraction pattern of TiO_2 which was characterized using an XRD tool with five peaks visible in the graph which will be described in Table 1.

The following is a table of results for each peak intensity and angle of 2θ TiO_2 .

Table 1. Results of each peak intensity and angle of 2θ TiO_2

Pos. [$^{\circ}2\theta$.]	h k l	Crystal Size (nm)	Lattice Constants						Crystal Structure
			a (\AA)	b (\AA)	c (\AA)	α ($^{\circ}$)	β ($^{\circ}$)	γ ($^{\circ}$)	
27,441	1 1 0	93,158	4,594	4,594	2,958	90	90	90	Tetragonal
36,063	1 0 1	93,158	4,594	4,594	2,958	90	90	90	Tetragonal
41,235	1 1 1	96,683	4,594	4,594	2,958	90	90	90	Tetragonal
54,292	2 1 1	96,683	4,594	4,594	2,958	90	90	90	Tetragonal
68,991	3 0 1	114,54	4,594	4,594	2,958	90	90	90	Tetragonal

Figure 1 is a TiO_2 diffraction pattern tested using an XRD device. From Figure 1 it produces data such as those in Table 1. It can be seen in Table 1 that there are five highest peaks. The results of Table 1 obtained Tetragonal structure for the whole TiO_2 . By using Equation (1) obtained crystal size with an average of 98.9 nm.

The following is data on the characterization of cassava peel activated carbon using an XRD tool.

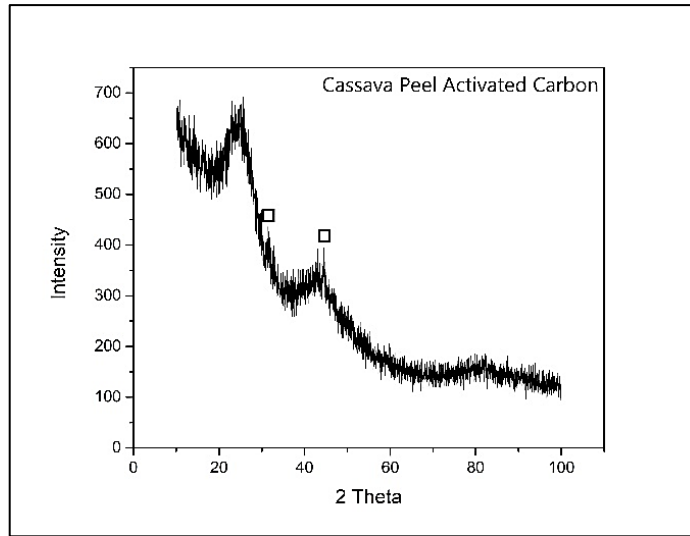


Figure 2. Diffraction pattern of cassava peel activated carbon

Figure 2 is a graph of the diffraction pattern of cassava peel activated carbon which was characterized using an XRD tool with two peaks visible in the graph which will be described in Table 2. The following is a table of results for each peak intensity and angle of 2θ cassava peel activated carbon.

Table 2. Results of each peak intensity and 2θ angle of cassava peel activated carbon

Pos. [^o 2Th.]	h k l	Crystal Size (nm)	Lattice Constants						Crystal Structure
			a (Å)	b (Å)	c (Å)	α (^o)	β (^o)	γ (^o)	
31,539	0 0 2	17,467	2,464	2,464	6,736	90	90	120	Hexagonal
44,482	1 0 1	23,289	2,464	2,464	6,736	90	90	120	Hexagonal

Figure 2 is the diffraction pattern of cassava peel activated carbon tested using XRD. From Figure 2 it produces data such as those in Table 2. It can be seen in Table 2 that there are two highest peaks. The results from Table 2 obtained Hexagonal structure for both carbons and by using Equation (1) obtained crystal size with an average of 20.4 nm.

The following is data on the characterization of TiO₂/Cassava peel activated carbon nanocomposites with variations of 40%:60% using an XRD tool.

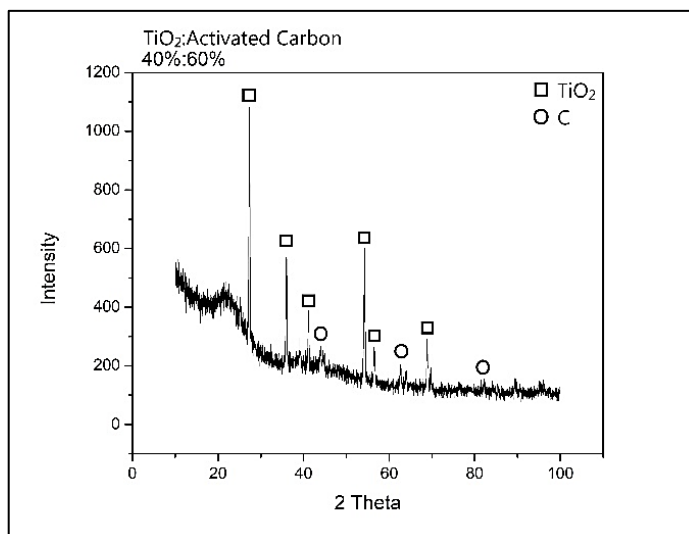


Figure 3. Diffraction Pattern of TiO_2 /Activated Carbon Cassava Skin Nanocomposite Variation 40%:60%

Figure 3 is a graph of the diffraction pattern of TiO_2 /Activated Carbon Cassava Skin Nanocomposite Variation 40%:60% which was characterized using an XRD tool with nine peaks visible in the graph which will be described in Table 3. The following is a table of results for each peak intensity and angle of 2θ TiO_2 /Activated Carbon Cassava Skin Nanocomposite Variation 40%:60%.

Table 3. Results of Each Peak Intensity and Angle of 2θ TiO_2 /Activated Carbon Cassava Skin Nanocomposite Variation 40%:60%

Pos. [2θ]	h k l	Crystal Size (nm)	Lattice Constants						Crystal Structure	Phase
			a (Å)	b (Å)	c (Å)	α ($^\circ$)	β ($^\circ$)	γ ($^\circ$)		
27,365	1 1 0	55,912	4,600	4,600	2,965	90	90	90	Tetragonal	TiO_2
35,983	1 0 1	55,912	4,600	4,600	2,965	90	90	90	Tetragonal	TiO_2
41,184	1 1 1	79,859	4,600	4,600	2,965	90	90	90	Tetragonal	TiO_2
43,943	2 1 0	55,899	3,567	3,567	3,567	90	90	90	Cubic	C
54,202	2 1 1	79,859	4,600	4,600	2,965	90	90	90	Tetragonal	TiO_2
56,552	2 2 0	55,912	4,600	4,600	2,965	90	90	90	Tetragonal	TiO_2
63,943	3 1 0	39,929	2,456	2,456	10,04	90	90	120	Rhombohedral	C
68,881	3 0 1	55,912	4,600	4,600	2,965	90	90	90	Tetragonal	TiO_2
82,146	3 2 1	46,579	2,522	2,522	43,24	90	90	120	Rhombohedral	C

Figure 3 is the diffraction pattern of the TiO_2 /Activated carbon cassava skin nanocomposite variation of 40%:60% tested using an XRD tool. Figure 3 produces data as in Table 3. It can be seen in Table 3 that there are nine highest peaks. The results from Table 3 show a Tetragonal structure for all TiO_2 , while Cubic and Rhombohedral for carbon. By using Equation (1), the

average crystal size is 58.4 nm. The following is data on the characterization of TiO₂/Cassava peel activated carbon nanocomposites with variations of 50%:50% using an XRD tool.

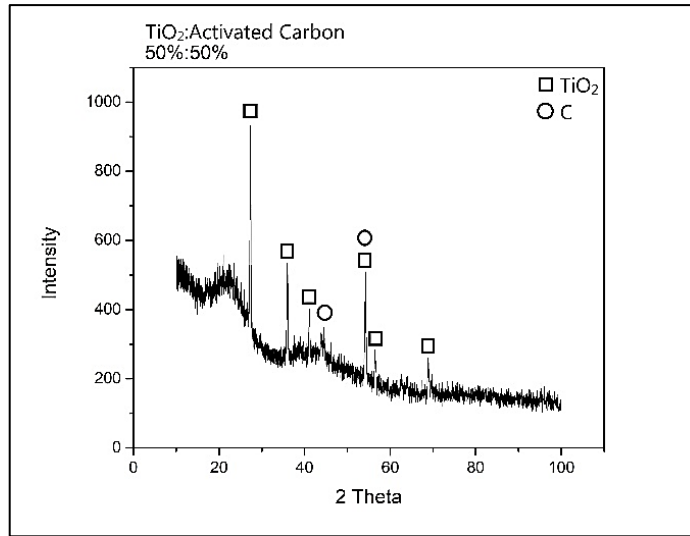


Figure 4. Diffraction Pattern of TiO₂ Nanocomposite/Activated Carbon Cassava Skin Variation 50%:50%

Figure 4 is a graph of the diffraction pattern of TiO₂/Activated Carbon Cassava Skin Nanocomposite Variation 50%:50% which was characterized using an XRD tool with eight peaks visible in the graph which will be described in Table 4. The following is a table of results for each peak intensity and angle of 2θ TiO₂/Activated Carbon Cassava Skin Nanocomposite Variation 50%:50%.

Table 4. Results of each peak intensity and angle of 2θ TiO₂/Activated Carbon Cassava Skin Nanocomposite Variation 50%:50%

Pos. [°2Th.]	h k l	Crystal Size (nm)	Lattice Constants						Crystal Structure	Phase
			a (Å)	b (Å)	c (Å)	α (°)	β (°)	γ (°)		
27,359	1 1 0	79,859	4,600	4,600	2,965	90	90	90	Tetragonal	TiO ₂
35,977	1 0 1	69,882	4,600	4,600	2,965	90	90	90	Tetragonal	TiO ₂
41,166	1 1 1	93,158	4,600	4,600	2,965	90	90	90	Tetragonal	TiO ₂
43,901	2 1 0	46,579	2,470	2,470	6,800	90	90	120	Hexagonal	C
54,268	2 1 1	69,882	4,600	4,600	2,965	90	90	90	Tetragonal	TiO ₂
54,268	2 1 1	69,882	2,470	2,470	6,800	90	90	120	Hexagonal	C
56,446	2 2 0	39,929	4,600	4,600	2,965	90	90	90	Tetragonal	TiO ₂
68,885	3 0 1	55,912	4,600	4,600	2,965	90	90	90	Tetragonal	TiO ₂

Figure 4 is the diffraction pattern of the TiO₂/Activated carbon cassava skin nanocomposite variation of 50%:50% tested using an XRD tool. Figure 4 produces data as in Table 4. It can be seen in Table 4 that there are eight highest peaks. The results from Table 4 show a Tetragonal structure for all TiO₂, while Hexagonal for carbon. By using Equation (1), the average crystal size

is 65.7 nm. The following is data on the characterization of TiO₂/Cassava peel activated carbon nanocomposites with variations of 60%:40% using an XRD tool.

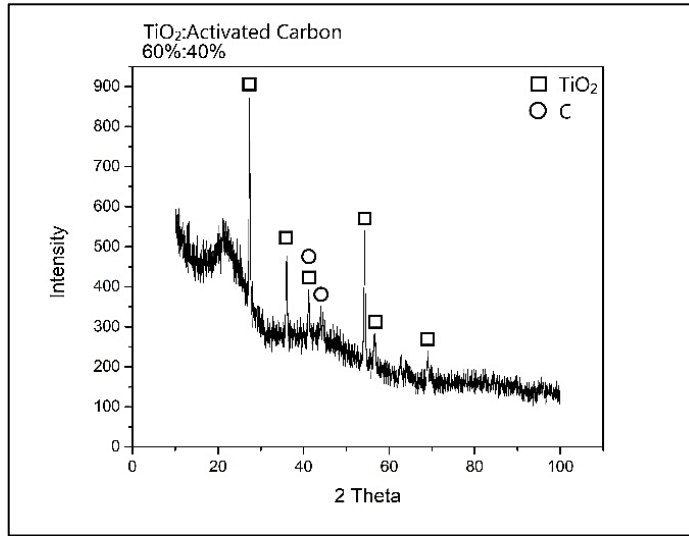


Figure 5. Diffraction Pattern of TiO₂/Activated Carbon Cassava Skin Nanocomposite Variation 60%:40%

Figure 5 is a graph of the diffraction pattern of TiO₂/Activated Carbon Cassava Skin Nanocomposite Variation 60%:40% which was characterized using an XRD tool with eight peaks visible in the graph which will be described in Table 5. The following is a table of results for each peak intensity and angle of 2θ TiO₂/Activated Carbon Cassava Skin Nanocomposite Variation 60%:40%.

Table 5. Results of each peak intensity and angle of 2θ TiO₂/Activated Carbon Cassava Skin Nanocomposite Variation 60%:40%

Pos. [°2Th.]	h k l	Crystal Size (nm)	Lattice Constants						Crystal Structure	Phase
			a (Å)	B (Å)	C (Å)	α (°)	β (°)	γ (°)		
27,394	1 1 0	111,77	4,594	4,594	2,959	90	90	90	Tetragonal	TiO ₂
36,039	1 0 1	69,882	4,594	4,594	2,959	90	90	90	Tetragonal	TiO ₂
41,237	1 1 1	39,929	4,594	4,594	2,959	90	90	90	Tetragonal	TiO ₂
41,237	1 1 1	39,929	12,38	12,38	12,38	90	90	90	Cubic	C
44,572	2 1 0	46,579	2,470	2,470	6,800	90	90	120	Hexagonal	C
54,236	2 1 1	139,68	4,594	4,594	2,959	90	90	90	Tetragonal	TiO ₂
56,650	2 2 0	46,579	4,594	4,594	2,959	90	90	90	Tetragonal	TiO ₂
27,394	1 1 0	111,77	4,594	4,594	2,959	90	90	90	Tetragonal	TiO ₂

Figure 5 is the diffraction pattern of the TiO₂/Activated carbon cassava skin nanocomposite variation of 50%:50% tested using an XRD tool. Figure 5 produces data as in Table 5. It can be seen in Table 5 that there are eight highest peaks. The results from Table 5 show a Tetragonal

structure for all TiO₂, while Cubic and Hexagonal for carbon. By using Equation (1), the average crystal size is 67.7 nm.

In tests using an XRD tool for three variations of TiO₂/Activated Carbon nanocomposites, different crystal structures and sizes were obtained. From the results obtained, the crystal size of three variations of TiO₂/Activated Carbon nanocomposites has a crystal size of <100 nm, therefore the three variations of TiO₂/Activated Carbon nanocomposites used in this research have met the requirements for nano size. Nanocomposites are defined as multi-phase materials, where each phase has one, two, or three dimensions of less than 100 nanometers (nm) [33]. In the results obtained, variations in mass composition affect the structure and size of the crystals. From the data that has been obtained, it can be seen that in the variation of the TiO₂/Activated Carbon nanocomposite variation of 60%:40% there is an increase in crystal size. The increase in crystal size in the TiO₂/Activated Carbon nanocomposite variation of 60%:40% is caused by the mass of TiO₂ being greater than the mass of active carbon because TiO₂ has a larger crystal size than active carbon. This is in accordance with research conducted by Zaldi & Ratnawulan [23] which states that variations in composition affect the structure and size of the crystals. In Aflahannisa & Astuti's research [5] obtained different crystal structure and size results for each variation of Carbon-TiO₂ composition. In Susana & Astuti's research [24] get different crystal size results for each variation of LiOH composition. Based on the lattice constants obtained, different edge lengths and angles are obtained because they have different crystal structures. The lattice constant for a Tetragonal structure has two equal and one different edge lengths ($a=b \neq c$) with equal angles ($\alpha=\beta=\gamma$) [34]. The lattice constant for a Cubic structure has the same edge lengths ($a=b=c$) with equal angles ($\alpha=\beta=\gamma$) [35]. The lattice constant for Orthorhombic structures has different edge lengths ($a \neq b \neq c$) with the same angles ($\alpha=\beta=\gamma$) [36]. The lattice constant for a Hexagonal structure has two equal and one different edge lengths ($a=b \neq c$) with two equal and one different angles ($\alpha=\beta \neq \gamma$) [37]. The lattice constant for a Rhombohedral structure has two equal and one different edge lengths ($a=b \neq c$) with two equal and one different angles ($\alpha=\beta \neq \gamma$) [38].

4. Conclusion

This research was conducted to determine the structure and crystal size of variations in the mass composition of TiO₂/Cassava peel activated carbon nanocomposites using an XRD tool. The results of this research show that the structure and size of the crystal will be influenced by the variation, composition and mass used in its manufacture because each material used has a different crystal structure and size. For the TiO₂/Activated Carbon cassava peel nanocomposition, variations of 40%:60% obtained a crystal size of 58.4 nm with lattice constants $a=b=4.6001$ $c=2.9654$ and $\alpha=\beta=\gamma=90^\circ$ for the Tetragonal structure, $a=b=c=3.5670$ and $\alpha=\beta=\gamma=90^\circ$ for Cubic structure, and $a=b=2.4560$; 2.5221 $c=10.0440$; 43.2450 for Rhombohedral structure. For the TiO₂/Cassava peel activated carbon nanocomposition, variations of 50%:50% obtained a crystal size of 65.7 nm with lattice constants $a=b=4.6001$ $c=2.9654$ and $\alpha=\beta=\gamma=90^\circ$ for Tetragonal and a structures. $a=b=2.4700$ $c=6.8000$ and $\alpha=\beta=90^\circ$ $\gamma=120^\circ$ for Hexagonal structure. For the TiO₂/Cassava peel activated carbon nanocomposition, variations of 60%:40% obtained a crystal size of 67.7 nm with lattice constants $a=b=4.5940$ $c=2.9590$ and $\alpha=\beta=\gamma=90^\circ$ for the Tetragonal structure, $a=b=c=12.380$ and $\alpha=\beta=\gamma=90^\circ$ for Cubic structures, and $a=b=2.4700$ $c=6.8000$ and $\alpha=\beta=90^\circ$ $\gamma=120^\circ$ for Hexagonal structures.

Acknowledgments

The author would like to thank the supervisors who have helped in carrying out this research. The author also thanks his family and friends who have provided support to the author.

References

- [1] M. Nasution, "Karakteristik Baterai Sebagai Penyimpan Energi Listrik Secara Spesifik," *JET (Journal Electr. Technol.*, vol. 6, no. 1, pp. 35–40, 2021, [Online]. Available: <https://jurnal.uisu.ac.id/index.php/jet/article/view/3797>
- [2] M. H. Fadhilah, E. Kurniawan, and U. Sunarya, "PERANCANGAN DAN IMPLEMENTASI MPPT CHARGE CONTROLLER PADA PANEL SURYA MENGGUNAKAN MIKROKONTROLER UNTUK PENGISIAN BATERAI SEPEDA LISTRIK," *e-Proceeding Eng.*, vol. 4, no. 3, pp. 3164–3170, 2017.
- [3] F. A. Perdana, "BATERAI LITHIUM," *INKUIRI J. Pendidik. IPA*, vol. 9, no. 2, pp. 103–109, 2020, doi: 10.20961/inkui.v9i2.50082.
- [4] S. Tamilselvi *et al.*, "A Review on Battery Modelling Techniques," *Sustain.*, vol. 13, no. 18, pp. 1–26, 2021, doi: 10.3390/su131810042.
- [5] Aflahannisa and Astuti, "Sintesis Nanokomposit Karbon-TiO₂ Sebagai Anoda Baterai Lithium," *J. Fis. Unand*, vol. 5, no. 4, pp. 357–363, 2016.
- [6] J. Ginting, E. Yulianti, and Sudaryanto, "SINTESIS Li₂TiO₃ SEBAGAI BAHAN ANODA BATERAI Li-ION DENGAN METODE REAKSI PADATAN," *J. Sains Mater. Indones.*, vol. 15, no. 4, pp. 196–200, 2014.
- [7] E. O. Miklicanin, A. Badnjevic, A. Kazagic, and M. Hajlovac, "Nanocomposite: a brief review," *Health Technol. (Berl.)*, vol. 10, pp. 51–59, 2020.
- [8] S. K. Kumar and R. Krishnamoorti, "Nanocomposites: Structure, Phase Behavior, and Properties," *Annu. Rev. Chem. Biomol. Eng.*, vol. 1, pp. 37–58, 2010, doi: 10.1146/annurev-chembioeng-073009-100856.
- [9] S. Komarneni, "Nanocomposites," vol. 2, no. 12, pp. 1219–1230, 1992.
- [10] A. Trenggono, S. Herbirowo, A. Milandia, and A. Sudradjat, "SINTESIS DAN KARAKTERISASI EPOKSI NANOKOMPOSIT BERPENGUAT Fe-Ni NANOPARTIKEL DENGAN VARIASI FRAKSI BERAT SERTA WAKTU SONIKASI," pp. 185–191.
- [11] Y. Suyono, "STUDI AWAL PEMBUATAN NANOKOMPOSIT DENGAN FILLER ORGANOCILAY UNTUK KEMASAN," *Biopropal Ind.*, vol. 3, no. 2, pp. 63–69, 2012.
- [12] I. Sriyanti, "Nanocomposite prepared by simple mixing method," *Proceeding Third Int. Semin. Sci. Educ.*, pp. 1–6, 2009.
- [13] Hadiyawardman, A. Rijal, B. W. Nuryadin, M. Abdullah, and Khairurrijal, "Fabrikasi Material Nanokomposit Superkuat, Ringan dan Transparan Menggunakan Metode Simple Mixing," vol. 1, no. 1, pp. 14–21, 2008.
- [14] I. Fatimah, "DISPERSI TiO₂ KE DALAM SiO₂-MONTMORILLONIT : EFEK JENIS PREKURSOR," vol. 14, no. 1, pp. 41–58, 2009.

- [15] R. Nurillahi, D. N. Halimah, D. G. Apriliani, and I. Fatimah, "PENGOLAHAN LIMBAH BATIK CAIR MENGGUNAKAN FOTOKATALIS TiO_2 -ABU VULKANIK DESA WUKIRSARI YOGYAKARTA," *Khazanah J. Mhs.*, vol. 10, no. 2, pp. 1–8, 2018, doi: 10.20885/khazanah.vol10.iss2.art3.
- [16] A. R. Permatasari, L. U. Khasanah, and E. Widowati, "KARAKTERISASI KARBON AKTIF KULIT SINGKONG (Manihot utilissima) DENGAN VARIASI JENIS AKTIVATOR," *J. Teknol. Has. Pertan.*, vol. VII, no. 2, pp. 70–75, 2014, doi: 10.20961/jthp.v0i0.13004.
- [17] Z. Heidarinejad, M. H. Dehghani, M. Heidari, G. Javedan, I. Ali, and M. Sillanpaa, "Methods for preparation and activation of activated carbon: a review," *Environ. Chem. Lett.*, vol. 18, no. 2, pp. 393–415, 2020, doi: 10.1007/s10311-019-00955-0.
- [18] L. M. Yuningsih, D. Mulyadi, and A. J. Kurnia, "Pengaruh Aktivasi Arang Aktif dari Tongkol Jagung dan Tempurung Kelapa Terhadap Luas Permukaan dan Daya Jerap Iodin," *J. Kim. Val.*, vol. 2, no. 1, pp. 30–34, 2016, doi: 10.15408/jkv.v2i1.3091.
- [19] Z. Efendi and Astuti, "Pengaruh Suhu Aktivasi Terhadap Morfologi dan Jumlah Pori KEfendi, Z., & Astuti. (2016). Pengaruh Suhu Aktivasi Terhadap Morfologi dan Jumlah Pori Karbon Aktif Tempurung Kemiri sebagai Elektroda. 5(4), 297–302.arbon Aktif Tempurung Kemiri sebagai Elektrod," vol. 5, no. 4, pp. 297–302, 2016.
- [20] Z. R. E. Ntelok, "LIMBAH KULIT SINGKONG (MANIHOT ESCULENTA L.): ALTERNATIF OLAHAN MAKANAN SEHAT," *J. Inov. Pendidik. Dasar*, vol. 1, no. 1, pp. 115–121, 2017.
- [21] M. E. Kosim, R. Siskayanti, D. Prambudi, and W. D. Rusanti, "PERBANDINGAN KAPASITAS ADSORPSI KARBON AKTIF DARI KULIT SINGKONG DENGAN KARBON AKTIF KOMERSIL TERHADAP LOGAM TEMBAGA DALAM LIMBAH CAIR ELECTROPLATING," *J. Redoks*, vol. 7, no. 1, pp. 36–47, 2022, [Online]. Available: <https://jurnal.univpgri-palembang.ac.id/index.php/redoks/article/view/6637%0Ahttps://jurnal.univpgri-palembang.ac.id/index.php/redoks/article/viewFile/6637/5960>
- [22] Ikawati and Melati, "PEMBUATAN KARBON AKTIF DARI LIMBAH KULIT SINGKONG UKM TAPIOKA KABUPATEN PATI," *Pembuatan Karbon Aktif Dari Limbah Kulit Singkong Ukm Tapioka Kabupaten Pati*, pp. 1–8, 2009.
- [23] D. Zaldi and Ratnawulan, "PENGARUH VARIASI KOMPOSISI TERHADAP UKURAN KRISTAL LAPISAN NANOKOMPOSIT $\text{MnO-Fe}_2\text{O}_3/\text{PS}$ SEBAGAI SELF CLEANING," *Pillar Phys.*, vol. 14, no. 1, pp. 32–40, 2021.
- [24] H. Susana and Astuti, "Pengaruh Konsentrasi LiOH terhadap Sifat Listrik Anoda Baterai Litium Berbasis Karbon Aktif Tempurung Kemiri," *Fis. Unand*, vol. 5, no. 2, pp. 136–141, 2016.
- [25] A. Suprabawati, Holiyah, N. Wiwi, and Jasmansyah, "Kulit Singkong (Manihot esculenta Crantz) Sebagai Karbon Aktif Dengan Berbagai Langkah Pembuatan untuk Adsorpsi Ion Logam Timbal (Pb^{2+}) dalam Air," *J. Kartika Kim.*, vol. 1, no. 1, pp. 21–28, 2018, doi: 10.26874/jkk.v1i1.8.
- [26] L. Maulinda, N. ZA, and D. N. Sari, "Pemanfaatan Kulit Singkong sebagai Bahan Baku Karbon Aktif," vol. 4, no. 2, pp. 11–19, 2015.

- [27] D. R. Eddy, A. R. Noviyanti, and D. Janati, "SINTESIS SILIKA METODE SOL-GEL SEBAGAI PENYANGGA FOTOKATALIS TiO_2 TERHADAP PENURUNAN KADAR KROMIUM DAN BESI," *J. Sains Mater. Indones.*, vol. 17, no. 2, pp. 82–89, 2016.
- [28] A. Listanti, A. Taufiq, A. Hidayat, and S. Sunaryono, "Investigasi Struktur dan Energi Band Gap Partikel Nano TiO_2 Hasil Sintesis Menggunakan Metode Sol-Gel," *JPSE (Journal Phys. Sci. Eng.*, vol. 3, no. 1, pp. 8–15, 2018, doi: 10.17977/um024v3i12018p008.
- [29] Sumari, Y. F. Prakasa, M. R. Asrori, and D. R. Baharintasari, "Analisis Kandungan Mineral Pasir Pantai Bajul Mati Kabupaten Malang Menggunakan XRF dan XRD," *Fuller. J. Chem.*, vol. 5, no. 2, pp. 58–62, 2020, doi: 10.37033/fjc.v5i2.154.
- [30] I. A. Mahmudi, "STUDI PENGUJIAN X-RAY DIFFRACTION (XRD) PADA ALUMINIUM SILIKON (Al-Si) DENGAN PERLAKUAN PANAS ARTIFICIAL AGING 200°C ," pp. 1–10, 2020, [Online]. Available: <https://core.ac.uk/download/pdf/196255896.pdf>
- [31] V. S. I. Negara and Astuti, "PENGARUH TEMPERATUR SINTERING KARBON AKTIF BERBASIS TEMPURUNG KEMIRI TERHADAP SIFAT LISTRIK ANODA BATERAI LITTIUM," *Fis. Univ. Andalas*, vol. 4, no. 2, pp. 178–184, 2015.
- [32] Masruroh, A. B. Manggara, T. Papilaka, and R. T. T, "Penentuan ukuran Kristal (crystallite size) lapisan tipis PZT dengan metode XRD melalui pendekatan persamaan Debye Scherrer," *Jur. Fis. dan Kim. FMIPA Univ. Brawijaya*, vol. 1, no. 2, pp. 24–29, 2013.
- [33] M. Marpaung, U. Ahmad, and N. Edhi S, "Pelapis Nanokomposit untuk Pengawetan Salak Pondoh Terolah Minimal," *J. Keteknikan Pertan.*, vol. 3, no. 1, pp. 73–80, 2015, doi: 10.19028/jtep.03.1.73-80.
- [34] P. W. K. Angraini and M. Hikam, "PENGUJIAN SIFAT FEROELEKTRIK FILM $\text{Ba}_{0,5}\text{Sr}_{0,5}\text{TiO}_3$ DOPING Nb_2O_5 (BNST)," *J. Sains Mater. Indones.*, vol. 0, no. 0, pp. 211–216, 2006, [Online]. Available: <http://jurnal.batan.go.id/index.php/jsmi/article/view/5171>
- [35] Y. Sarwanto, W. A. Adi, E. Sukirman, and A. Manaf, "ANALISIS FASA BAHAN MAGNETIK SISTEM $\text{Ba}_{1-x}\text{La}_x\text{O}_6\text{Fe}_2\text{O}_3$ ($0 < x < 0,7$)," *Pros. Pertem. Ilm. Pengetah. dan Teknol. Bahan 2012*, pp. 41–46, 2012.
- [36] H. Delvita, D. Djamas, and Ramli, "PENGARUH VARIASI TEMPERATUR KALSINASI TERHADAP KARAKTERISTIK KALSIUM KARBONAT (CaCO_3) DALAM CANGKANG KEONG SAWAH (Pila ampullacea) YANG TERDAPAT DI KABUPATEN PASAMAN," *Pillar Phys.*, vol. 6, pp. 17–24, 2015.
- [37] T. N. Marpaung and K. Sinulingga, "PENGARUH VARIASI SUHU TERHADAP KARAKTERISTIK STRUKTUR KRISTAL DAN MORFOLOGI LAPISAN NANO TiO_2 PADA PELAPISAN LOGAM ANTI KOROSI DENGAN METODE SOL - GEL SPIN COATING," vol. 8, no. 2, pp. 42–47, 2020.
- [38] M. C. Fajrah and V. Hadi, "Struktur Kristal CaCO_3 Berbahan Dasar Cakang Telur Ayam Ras Dengan Menggunakan Variasi Ukuran Butiran," vol. 23, no. 2, pp. 8–11, 2013.